


RESEARCH ARTICLE

WILEY

Analysis and design of asymmetric CLLC resonant DC-DC converter

Lei Sun¹  | Yuejin Ma¹ | Jing Wang¹ | Jianjun Hao¹ | Xuesong Suo¹ | Xiaoyu Li²

¹College of Mechanical and Electrical Engineering, Hebei Agricultural University, Baoding, China

²Key Laboratory of Distributed Energy Storage and Micro-Grid of Hebei Province, North China Electric Power University, Baoding, China

Correspondence

Lei Sun and Yuejin Ma, College of Mechanical and Electrical Engineering, Hebei Agricultural University, Baoding 071001, China.

Email: slsl0811@126.com (L. S.) and

Email: myj@hebau.edu.cn (Y. M.)

Funding information

Science and Technology Support Program of Baoding, Grant/Award Number: 18ZG011; Hebei Oil Plants Innovation Team in Modern Agricultural Industry Technology System; Natural Science Foundation of Hebei Province, Grant/Award Number: E2018502134; the project of "Energy Subsystem in Stratospheric satellite"

Peer Review

The peer review history for this article is available at <https://publons.com/publon/10.1002/2050-7038.12338>.

Summary

With the global climate deterioration and the increase of energy demands, distributed generation was used to converse the clean energy to electricity. Direct current–direct current (DC-DC) converter has been widely applied in many fields such as uninterruptible power supply (UPS) DC power distribution system, electric vehicles, and small photovoltaic power generation. Most of the CLLC resonant converters are of symmetric structures. However, asymmetric CLLC resonant converters are drawing more and more attention for higher voltage gain. But the operation characteristics of asymmetric CLLC resonant converters are more difficult to analyze, and the calculating method of the key parameters is also too complex. This paper analyzes the structure composition, operation principle, DC voltage gain, and frequency characteristics of the topology and then presents a method of parameter design to solve the key problem encountered in the asymmetric structure resonant converter design. By adopting the method of parameter design, it could be ensured that the converter has similar operation characteristics and a high transmission efficiency in both directions. Moreover, an asymmetric CLLC resonant DC-DC converter that connects 300-to-300-V DC and with a power rating of 1 kW is designed and built up to verify validity and correctness of this parameter design method.

KEYWORDS

CLLC, converter, parameters design

1 | INTRODUCTION

In the face of energy crisis, new and renewable energy and distributed generation system are drawing increasing attention. Direct current–direct current (DC-DC) converter can turn low-quality uncontrollable DC energy into high-quality

LIST OF SYMBOLS AND ABBREVIATIONS: β , ratio of actual load to full load; C_1 , C_2 , resonant capacitor; f_n , normalized frequency; f_p , first resonant frequency; f_r , second resonant frequency; f_s , working frequency; g , capacitance ratio; i_{C2} , resonant current in the reverse current; i_{Ds1} – i_{Ds4} , current antiparallel diodes; i_{Lm} , magnetizing current; i_{Lr} , resonant current in the forward direction; i_{S1} – i_{S8} , switch current; L_m , magnetizing inductance; L_r , resonant inductance; m , ratio of the magnetizing inductance to the resonant inductance; M , DC voltage gain; n , transformation ratio; Q_1 , quality factor in the forward direction; Q_2 , quality factor in the reverse direction; R_{ac} , AC equivalent resistance; S_1 – S_8 , MOSFET; u_{O1} – u_{O2} , output current; u_{gs1} – u_{gs8} , driving signal of switch; u_{S1} – u_{S8} , voltage between the drain and source of switch; u_{tank} , input voltage of the resonant tank; ω_r , angular frequency.

controllable DC energy in a new-energy system. So it is of great significance to study DC-DC converter for new and renewable power system.¹⁻³

High-power isolating-type bidirectional DC-DC converter can achieve variation of DC voltage, bidirectional transmission of energy, and electrical isolation, which has been widely applied into the fields such as uninterruptible power supply (UPS), DC power distribution system, and electric vehicles.⁴⁻⁸

In recent years, topologies of soft switching resonant DC-DC converter, especially LLC topologies, are drawing increasing attention from the world.⁹⁻¹³ LLC resonant converter was of natural soft switching properties, so the inverter switches achieve zero voltage switching (ZVS), and rectification switches achieve zero current switching (ZCS) without any auxiliary circuit.¹⁴⁻¹⁷ However, a lot of the current researches attach much importance to the unidirectional LLC resonant converter.

In order to improve the performance of resonant converters, Severns proposed 38 kinds of resonant converter topologies including 17 kinds of LLC resonant converter topologies with three resonant elements according to different permutations and combinations.¹⁸ However, they did not provide detailed analysis of the topologies. The bidirectional flow of energy that can power load and provide power feedback to the power grid can be realized using bidirectional topologies, so the CLLC topologies, that is, bidirectional LLC topologies, are drawing increasing attention from the world.¹⁹⁻²¹

So far, the bidirectional LLC resonant converter has not been fully investigated, and many of the topology researches focused on the fourth LLC topology (type-4 LLC). Sun et al proposed a design method based on phase sequence of LLC resonant converter,²² and Lv et al proposed a novel operation mode analysis for CLLC resonant converter.²³ However, they both focused on type-4 LLC topology. The researches on other bidirectional topologies such as type-11 LLC are incomplete. Type-11 LLC has a higher gain than type-4 LLC. However, there will be five resonant elements at least in symmetrical bidirectional topologies, and there will be only four resonant elements in asymmetric bidirectional topologies,²⁴ so its difficulty of parameters design is lower than five resonant elements design.²⁵

Asymmetric bidirectional topologies are regarded as kind of more flexible and efficient topologies. However, there is no grounding breaking achievement made in terms of the research on asymmetric bidirectional topologies because it is difficult to find a method of parameter design to endow the converter with a similar bidirectional operation characteristic. The topologies of type-4 LLC and type-11 LLC are shown in Figure 1.

In this paper, a bidirectional asymmetric CLLC resonant DC-DC converter was analyzed, and then, a method of parameter design to solve the key problem involved in the type-4 and type-11 LLC asymmetric structure resonant converter design was presented, so that the asymmetric CLLC resonant converter had a similar bidirectional operation characteristic and a high transmission efficiency. Moreover, an asymmetric CLLC resonant DC-DC converter that connected 300-to-300-V DC and with a power rating of 1 kW was designed and built up to verify validity and correctness of this parameter design method.

2 | TOPOLOGY STRUCTURE ANALYSIS

Bidirectional full-bridge CLLC resonant converter is shown in Figure 2. The asymmetric CLLC resonant tank is composed of type-4 LLC and type-11 LLC. These two full bridge converters are composed of MOSFET S_1 to S_4 and S_5 to S_8 . In the forward direction, S_1 , S_4 and S_2 , S_3 switch into conduction by turns in 50% duty cycle to achieve inversion. S_5 to S_8 will achieve rectification with their antiparallel diodes.

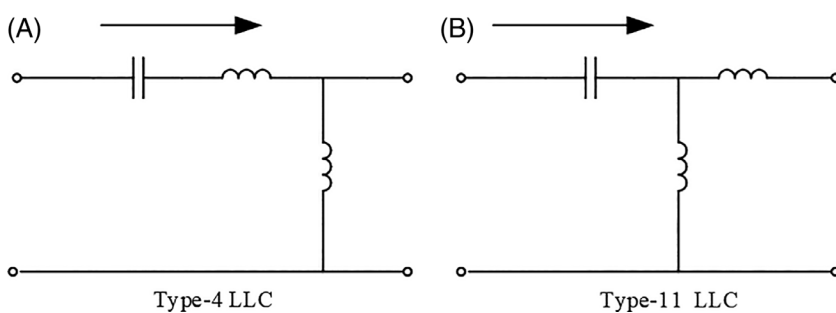


FIGURE 1 The topologies of type-4 LLC and type-11 LLC

There are eight stages of one operation period of the resonant converter. In the forward direction and reverse direction, the operating situations of the driving circuit are the same, and only the resonant elements are different from others. So the operating principles of the converter are basically the same, and it is only necessary to analyze one operating direction. When the converter operates in the forward direction, it is similar to the type-4 LLC, which has been studied in lots of papers such as Chen and Lu,⁷ so we will not analyze the forward direction. In this paper, the reverse direction was taken as an example to discuss the processes of the converter. The waveform of the converter that runs in the reverse direction is shown in Figure 3.

It is assumed that the converter runs stably and then, the equivalent circuit of the converter in each of the operating process can be achieved, shown in Figure 4.

t_0 denotes a transient time, and the previous period is over in t_0 to t_1 ; t_1 denotes the beginning of the new period. The detailed operating processes of the half cycle for reverse direction are shown in the following text:

Stage 1 (t_1 - t_2): The voltage across S_6 and S_7 decreases to 0 and gets turn-on signal at the time of t_0 , so S_6 and S_7 turn on under ZVS condition. The value of magnetizing inductance L_m is more than thrice the value of resonant inductance L_r in CLLC resonant converter, so it is assumed that the resonant tank consists of L_r , C_1 , and C_2 . The resonant current i_{C2} increases to sinusoidal wave.

Stage 2 (t_2 - t_3): In the previous stage, magnetizing current i_{Lm} is increasing linearly, after reaching the peak, and i_{C2} will decrease continually. At the time of t_2 , i_{Lm} will equal i_{C2} ; it means that there is no current in the transformer. The rectified current in secondary side decreases to 0. S_1 and S_4 are turned off under ZCS condition. In this stage, the resonant tank consists of L_m and C_2 .

Stage 3 (t_3 - t_4): S_6 and S_7 are turned off at the time of t_3 , and then, the resonant current i_{C2} will charge up the parasitic capacitances of S_6 and S_7 and discharge the parasitic capacitances of S_5 and S_8 .

Stage 4 (t_4 - t_5): After the parasitic capacitances of S_5 and S_8 complete discharge, i_{C2} feed back to the input terminal through the antiparallel diodes of S_5 and S_8 . After a while, S_2 and S_3 are turned on, and L_r and C_1 participate in the resonant of primary side. S_5 and S_8 are turned on under ZVS condition at the time of t_5 . It marks the end of the previous half cycle and the beginning of the second half cycle. The processes of the second half cycle are symmetry for the previous half cycle, so it is unnecessary to go into details.

By analyzing the operating processes, it can be known that the CLLC resonant converter can achieve ZVS in the primary side and ZCS in the secondary side.

3 | RESONANT PARAMETERS DESIGN AND ANALYSIS

3.1 | Resonant parameters design

In order to ensure a high power transmission efficiency, the converter will be specially arranged, and it will work near the resonant frequency. Under this condition, the current waveform is approximating sinusoidal waveform, so the fundamental harmonic approximation (FHA) is adopted to analyze it in this paper. The equivalent circuit in both directions is shown in Figure 5.

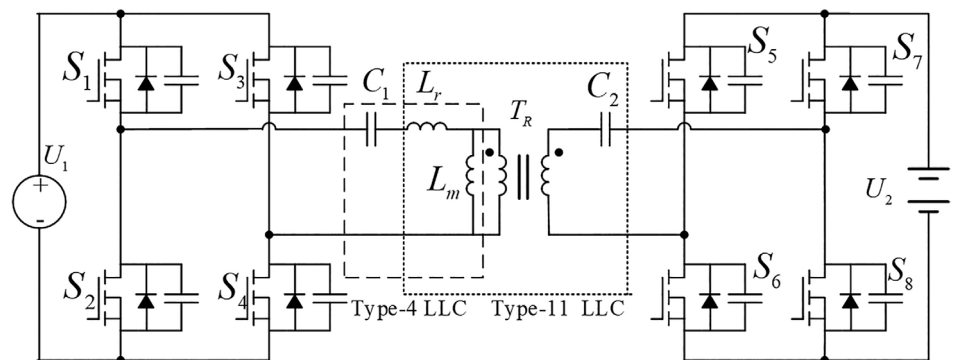


FIGURE 2 The topology of CLLC resonant converter

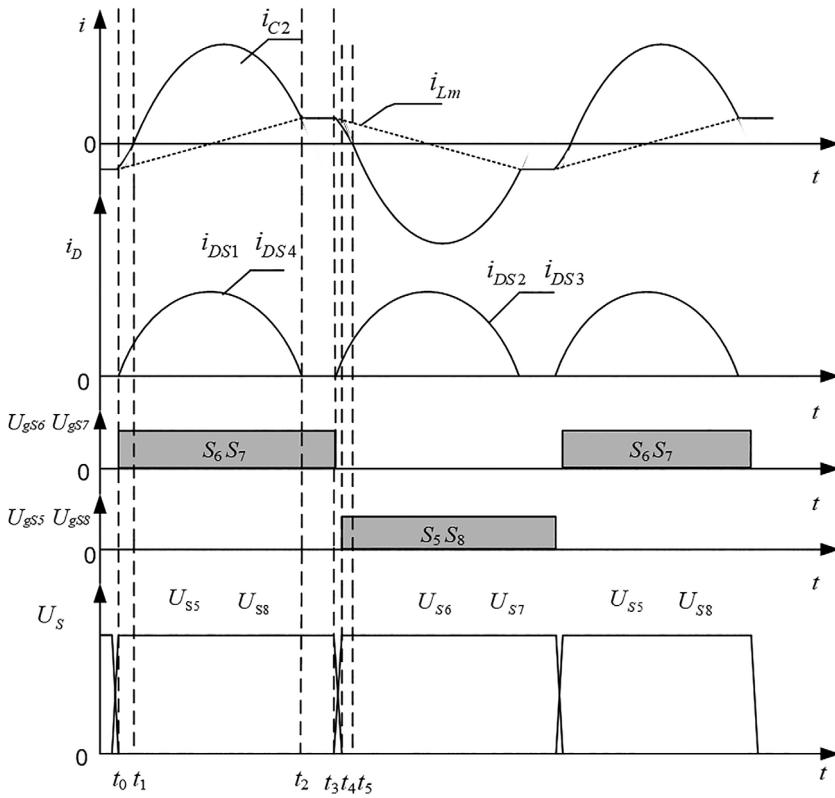


FIGURE 3 Waveform in a half switching cycle for reverse direction

In order to ensure good operating characteristics, the converter should have the same resonant converter in both directions. When fully loaded, the output terminal can be seen as short circuit. Then, the state equations in both directions in the second resonant frequency f_r can be obtained, as shown in Equations (1) and (2).

$$\begin{cases} -j\frac{1}{\omega_r C_1} + j\omega_r L_r + \frac{j\omega_r L_m \cdot \left(-j\frac{1}{\omega_r n^2 C_2}\right)}{j\omega_r L_m - j\frac{1}{\omega_r n^2 C_2}} = 0 \\ f_r = \frac{\omega_r}{2\pi} \end{cases} \quad (1)$$

$$\begin{cases} -j\frac{1}{\omega_r C_2} + \frac{j\omega_r L_m \cdot \left(j\omega_r n^2 L_r - j\frac{1}{\omega_r C_1/n^2}\right)}{j\omega_r L_m + j\omega_r n^2 L_r - j\frac{1}{\omega_r C_1/n^2}} = 0 \\ f_r = \frac{\omega_r}{2\pi} \end{cases} \quad (2)$$

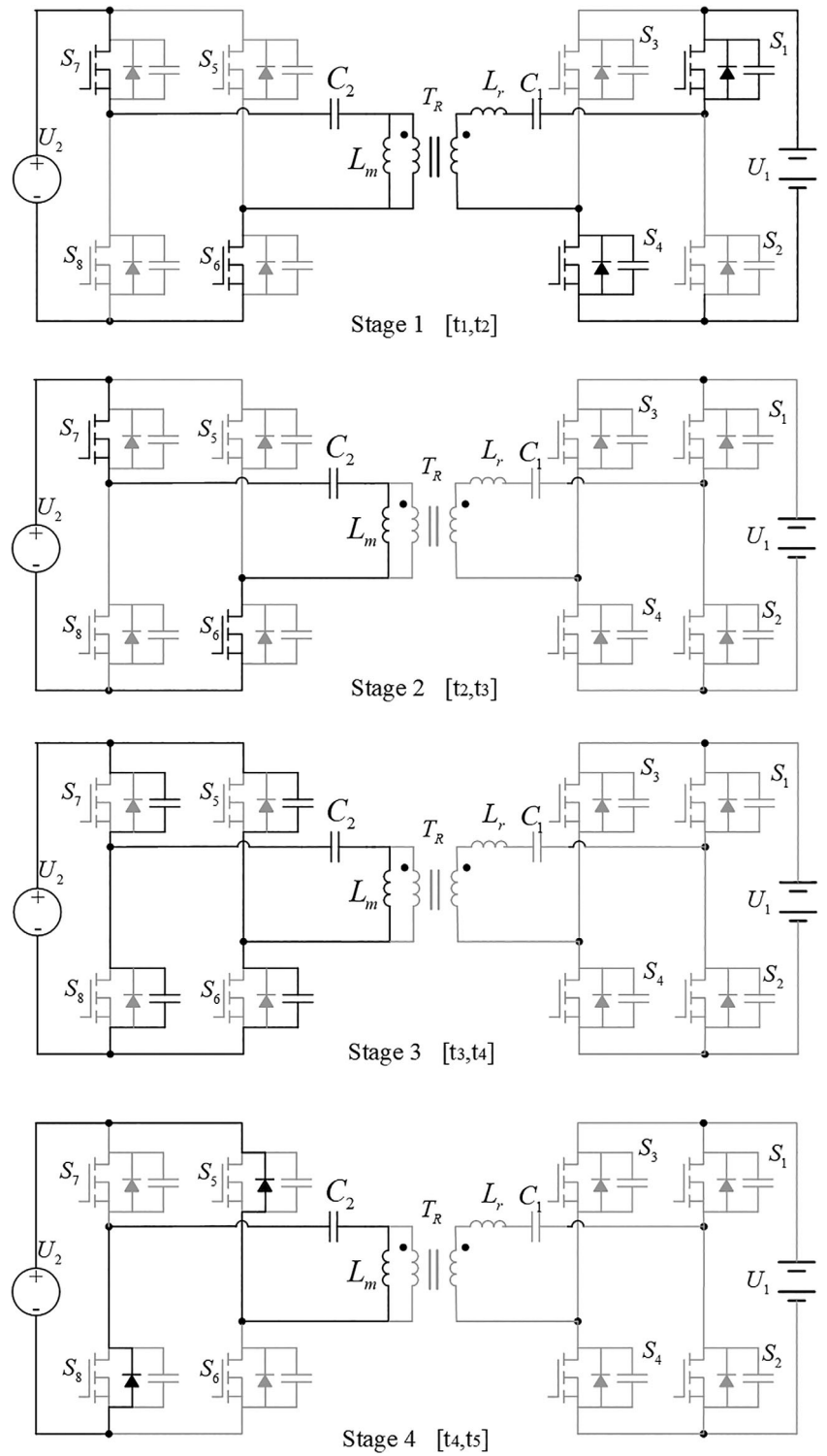
By simplifying Equations (1) and (2), the state equations can be obtained, as shown in Equations (3) and (4).

$$(2\pi f_r)^4 \cdot (C_1 C_2 L_m L_r) - (2\pi f_r)^2 (L_r C_1 + L_m C_1 + L_m n^2 C_2) + 1 = 0 \quad (3)$$

$$(2\pi f_r)^4 \cdot (C_1 C_2 L_m L_r) - (2\pi f_r)^2 (L_r C_1 + L_m C_1/n^2 + L_m C_2) + 1 = 0 \quad (4)$$

When there is no load, the output terminal can be seen as open circuit. Then, the state equations in both directions in the first resonant frequency f_p can be obtained, as shown in Equations (5) and (6).

FIGURE 4 Equivalent circuits of each stage for reverse direction



$$f_p = \frac{1}{2\pi\sqrt{(L_r + L_m)C_1}} \quad (5)$$

$$f_p = \frac{1}{2\pi\sqrt{L_m C_2}} \quad (6)$$

Transformer ratio n , the first resonant frequency f_p , and the second resonant frequency f_r are known quantities that can be substituted in the simultaneous Equations (3) to (6). Then, the values of L_r , L_m , C_1 , and C_2 can be worked out by the computation software.

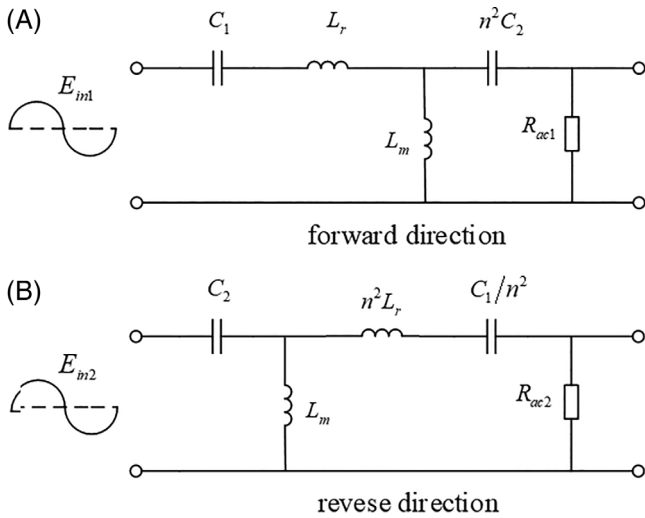


FIGURE 5 Fundamental wave equivalent circuits under both directions

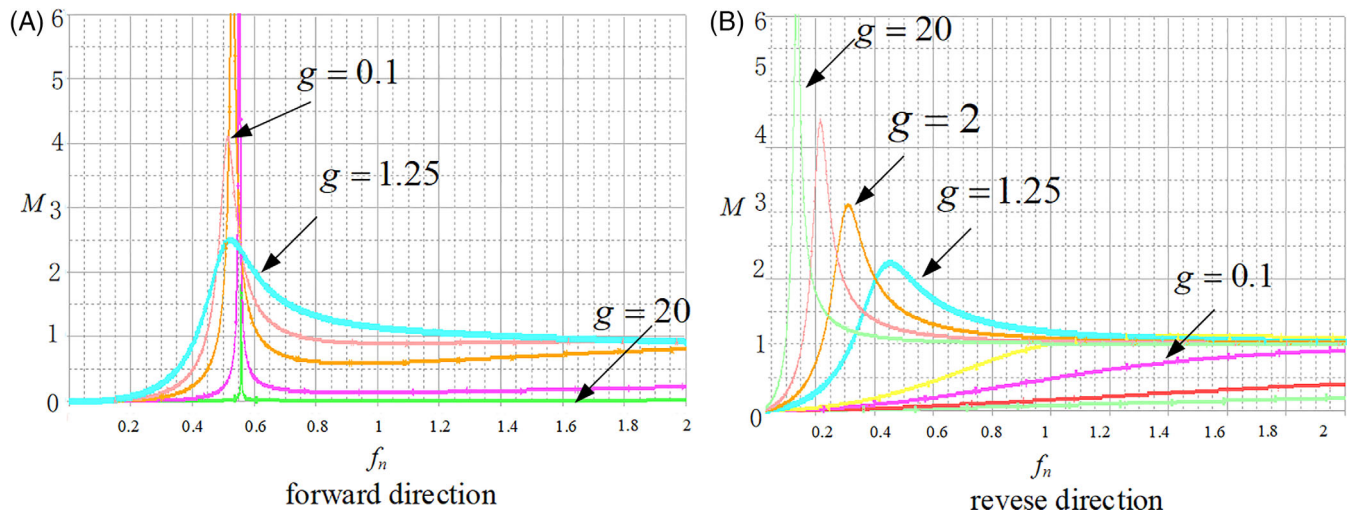


FIGURE 6 Direct current (DC) voltage gain waveforms for different g

In the resonant tank, the magnetizing inductance L_m to the resonant inductance L_r ratio $m = L_m/L_r$ and the capacitance ratio $g = C_2/C_1$ can be defined. Combining Equations (5) and (6), the capacitance ratio $g = 1 + 1/m$ and the normalized frequency $f_n = f_s/f_r$ can be obtained. Comparing Figure 5 with Figure 1, it can be concluded that the CLLC resonant converter has an additional capacitance under both directions compared with type-4 LLC and type-11 LLC, so the value of the capacitance ratio g is very important to the converter. As known quantity of design, in this paper, the values $n = 1$ and $m = 4$ were used; then, the DC voltage gain waveforms for different g were obtained, as shown in Figure 6. The DC voltage gain M is the ratio of the output voltage to the input voltage that is converted to second side.

In order to enhance the efficiency, the converter work is always made near the second resonant frequency f_r , which is also called $f_n = 1$. When it is applied in the industrial manufacture, the range of the normalized frequency f_n is usually designed as $f_n \in [0.6, 1.2]$. Make sure that the DC voltage gain $M > 1$ within the range and then high transmission efficiency can be obtained. As shown in Figure 6, when g increases, the inflection point in the forward direction will shift to the right while the inflection point in the reverse direction will shift to the left. The gain characteristics waveforms in both directions are so different. A value of g should be found to ensure the gain characteristics waveforms similar in both directions. Using the method proposed in this paper, $g = 1 + 1/m = 1.25$ can be obtained. As shown in Figure 6, the converter has similar gain characteristics waveforms in both directions when $g = 1.25$. It can be proved that the converter can achieve bidirectional operating in the same characteristic and the DC voltage gain $M > 1$ in the normal operating range, which suggests that the method proposed in this paper is effective.

3.2 | Resonant parameters design

Direct current voltage gain waveforms for different load ratio β (the ratio of actual load to full load) are shown in Figure 7. It can be seen that when the load ratio increases, the inflection point (the first resonant frequency) will shift to the left and the DC voltage gain will decrease. In the forward direction, the DC voltage gain $M = 1$ in the second resonant frequency f_r can be guaranteed under the over load condition as the method proposed in this paper. It means that, with the normal frequency, the CLLC converter can operate with a wide range load. As seen in Figure 7, in the reverse direction, using the method proposed in this paper can ensure the DC voltage gain $M = 1.2$ in the second resonant frequency f_r with full load. It means that in the normal load range, the converter has a high transmission efficiency.

In the resonant tank, some parameters are defined as follows:

$$Q_1 = \frac{\sqrt{L_r/C_1}}{R_{ac1}}, \quad (7)$$

$$Q_2 = \frac{\sqrt{n^2 L_r/C_2}}{R_{ac2}}, \quad (8)$$

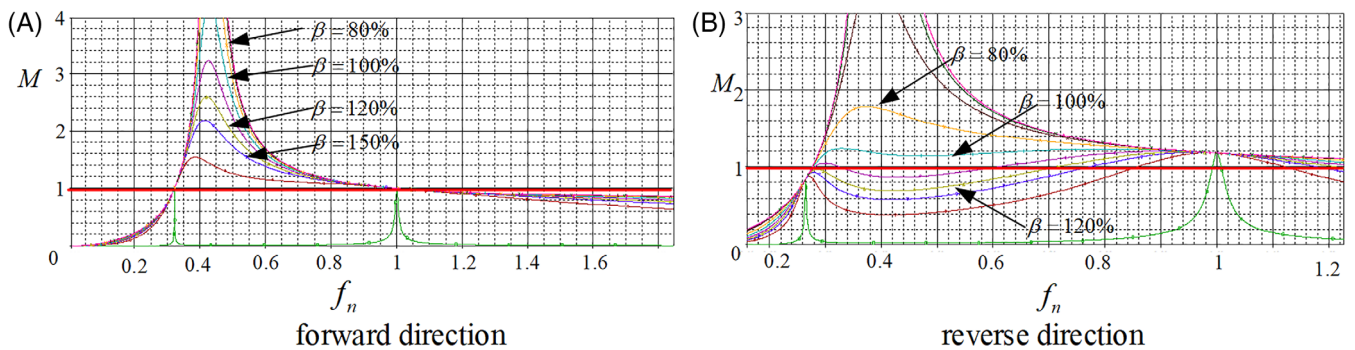


FIGURE 7 Direct current (DC) voltage gain waveforms for different load ratio β

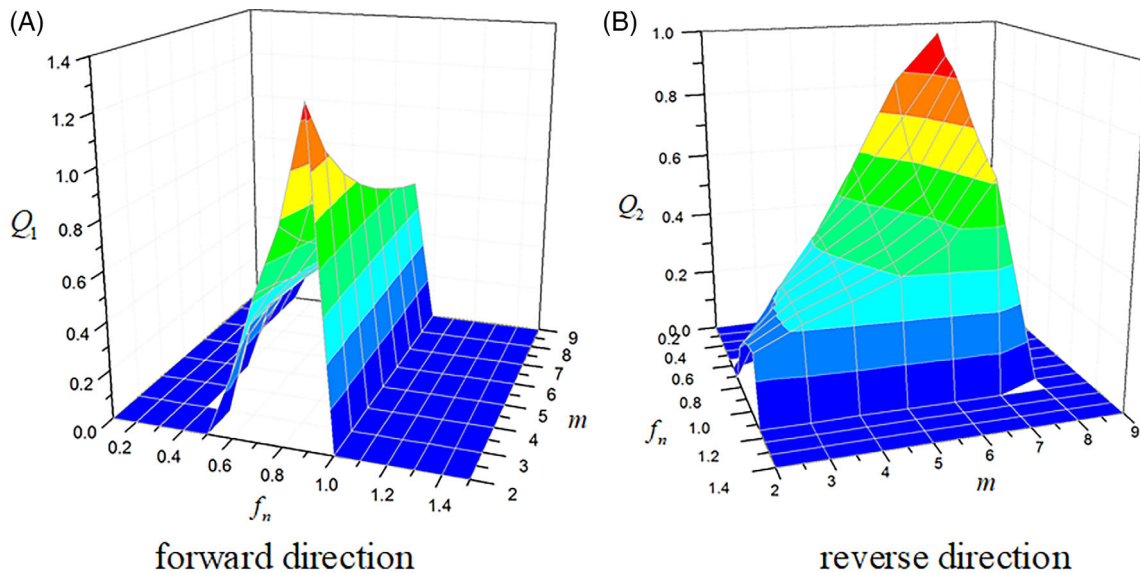


FIGURE 8 The relationship of Q , f_n , and m

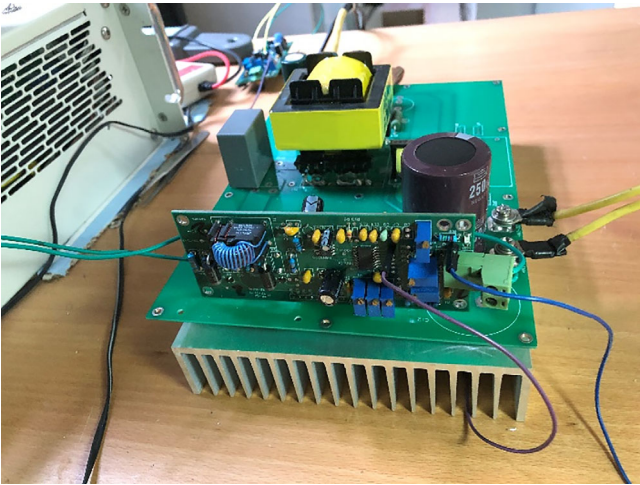


FIGURE 9 The prototype of CLLC resonant direct current–direct current (DC-DC) converter

Parameter	Value
Resonant inductor L_r	119 μH
Magnetic inductor L_m	476 μH
Resonant capacitor C_1	22 nF
Resonant capacitor C_2	28 nF
Transformation ratio n	28:28
First resonant frequency	50 kHz
Second resonant frequency	100 kHz

TABLE 1 The main parameters of the prototype

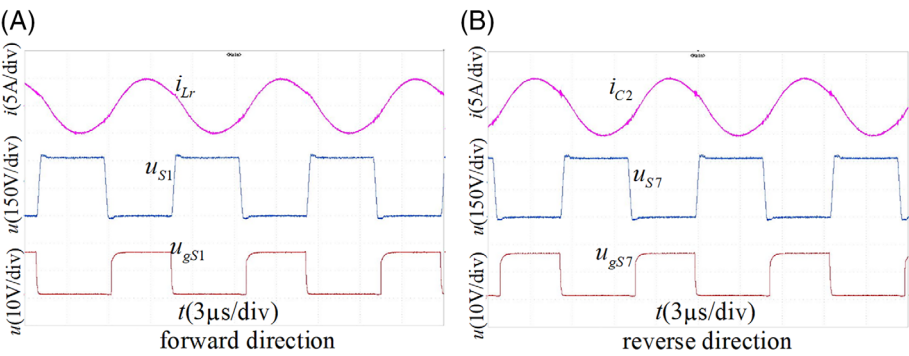


FIGURE 10 The resonant current and driving voltage with full load

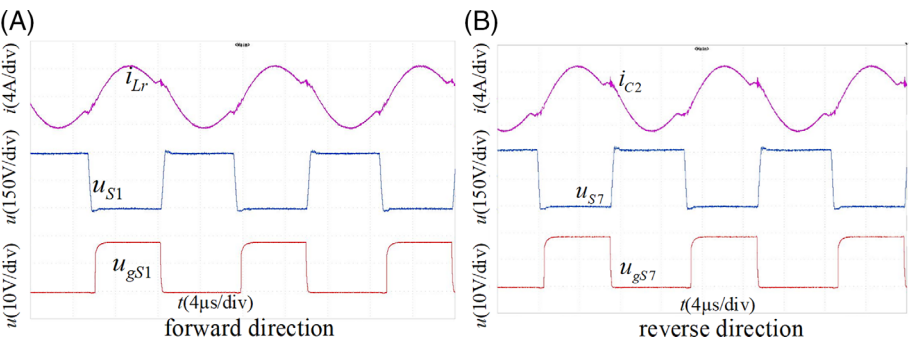


FIGURE 11 The resonant current and driving voltage with heavy load

FIGURE 12 The resonant current and voltage with heavy load

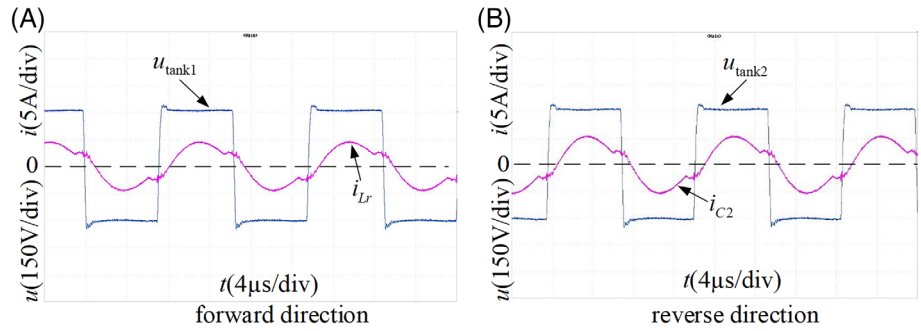
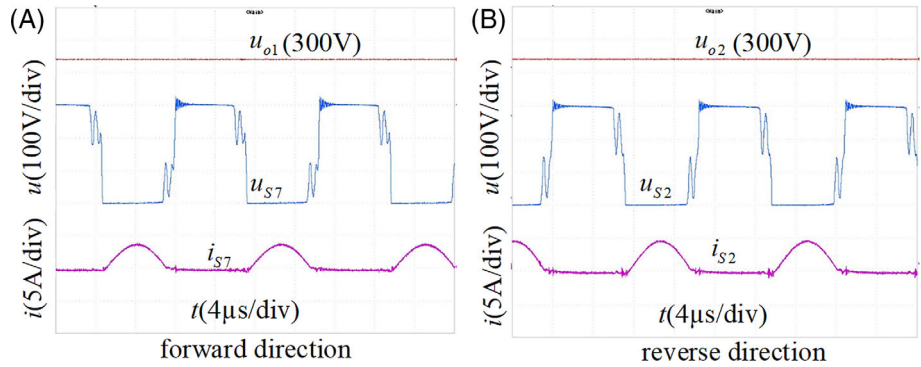


FIGURE 13 The voltage and current in secondary side with heavy load



$$R_{ac} = \frac{8n^2 U_o^2}{\pi^2 P_o}. \quad (9)$$

Q_1 : Quality factor in the forward direction;

Q_2 : Quality factor in the reverse direction;

R_{ac} : AC equivalent resistance.

In industrial manufacturing, in most cases, the quality factor is less than 1 to make sure that the converter safety is of low electrical stress. As we know, quality factor is proportional to the load ratio, and from Figure 7 and the analysis of Section 3.1, it can be concluded that the quality factor Q , the inductance ratio m , and normalized frequency f_n display mathematical relationship. So their expressions can be calculated simultaneously by the computation software; their relationship shown in Figure 8 can be obtained. From Figure 8, it is seen that the quality factors of the CLLC converter, which are designed by using the method proposed in this paper, are less than 1. It proves that the design method is a safe method.

4 | EXPERIMENT ANALYSIS

In order to verify the correctness of the design method proposed in this paper, an asymmetric CLLC resonant DC-DC converter that interfaces 300-to-300-V DC and with a power rating of 1 kW was designed, as shown in Figure 9. SiC MOSFET was used as switch for its high switching speed and low reverse recovery, which can reduce the switching loss obviously.

The main parameters of the prototype are shown in Table 1.

By changing the transformation ratio of the converter based on the design method proposed in this paper, they can be used in different occasions. The prototype designed in this paper is used for charging and discharging system of electric vehicles to realize 1:1 DC-DC electric isolation.

The experiment results are shown in Figures 10 to 13.

u_{gs} denotes the driving signal of switch; u_s denotes the voltage between the drain and source of switch; u_{tank} denotes the input voltage of the resonant tank; i_{Lr} denotes the resonant current in the forward direction; i_{C2} denotes the resonant current in the reverse current. As shown in Figure 10, when the converter runs in the second resonant frequency

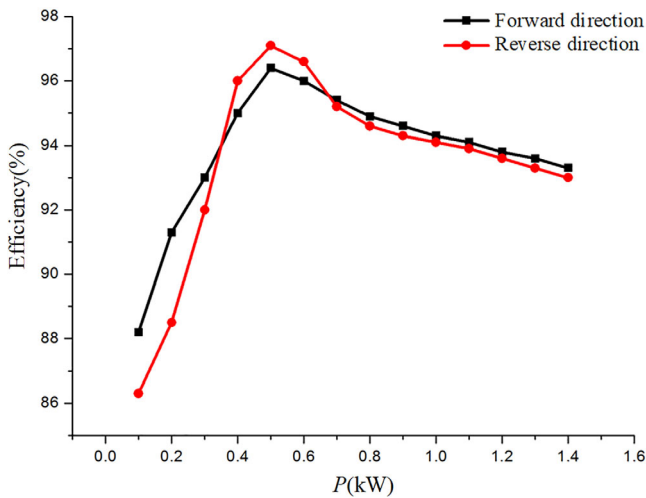


FIGURE 14 The efficiency waveforms in both directions

f_r with full load, the resonant current is a sinusoidal waveform, and it suggests that the method of resonant frequency computing is correct. From Figure 11, it can be seen that the experiment results are identical to the theoretical waveforms. From Figures 11 and 12, it can be seen that the voltage stress of u_{gS1} and u_{gS2} can be about 18 V, which can turn the MOSFET on. The voltage stress of u_{S1} and u_{S2} can reach 300 V that can meet the design requirement. As shown in Figure 12, the input voltage of the resonant tank u_{tank} decreases to 0 earlier than the resonant current. u_{O1} and u_{O2} are stabilized at 300 V. It means that the output voltage can meet the design requirement in both directions. Therefore, the primary side of the CLLC converter achieves ZVS in both directions. In Figure 13, the secondary side switch current i_S decreases to 0, and then, the voltage across switch u_S reaches high level, and the fact suggests that the secondary side of the CLLC converter achieves ZCS. The reverse recovery has been improved when SiC MOSFET is used.

The waveforms of the efficiency are shown in Figure 14. The peak efficiency in the reverse direction reaches 97.1%, and the peak efficiency in the forward direction reaches 96.3%. It can be concluded that the converter has higher efficiency in the reverse direction and good efficiency within wider load range in the forward direction. The correctness of Section 3.2 can be verified. The transmission efficiency of type-11 LLC in reverse direction is higher than type-4 LLC in forward direction.

5 | CONCLUSION

In this paper, a new bidirectional asymmetric CLLC resonant DC-DC converter was proposed and analyzed. The resonant converter can get a higher transmission efficiency in both of the two operating directions with only four resonant elements. By analyzing the influence of asymmetric structure on the DC voltage gain characteristics and transmission efficiency, a kind of parameters design method that helps realize similar operating characteristics in both directions was proposed. At last, a prototype was designed by using the method proposed in this paper, and the experiment results are positive and can be considered as evidence of the correctness and effectiveness of the design method.

ACKNOWLEDGEMENTS

This work is supported by Hebei Oil Plants Innovation Team in Modern Agricultural Industry Technology System, the Natural Science Foundation of Hebei Province (E2018502134), the Project of “Energy Subsystem in Stratospheric Satellite,” and Science and Technology Support Program of Baoding (18ZG011).

ORCID

Lei Sun  <https://orcid.org/0000-0003-0565-2000>

REFERENCES

1. Mohammadzadeh Shahir F, Babaei E, Sabahi M, Laali S. A new DC-DC converter based on voltage-lift technique. *International Transactions on Electrical Energy Systems*. 2016;26(6):1260-1286.

2. Babaei E, Saadatizadeh Z, Ranjbarizad V. A new nonisolated bidirectional DC-DC converter with ripple-free input current at low-voltage side and high conversion ratio. *International Transactions on Electrical Energy Systems*. 2017;27(1):e2494.
3. Babaei E, Abbasi O. A new topology for bidirectional multi-input multi-output buck direct current-direct current converter. *International Transactions on Electrical Energy Systems*. 2017;27(2):e2254.
4. Musavi F, Craciun M, Gautam DS, Eberle W, Dunford WG. An LLC resonant DC-DC converter for wide output voltage range battery charging applications. *IEEE Trans. on Power Electronics*. 2013;28(12):5437-5445.
5. Chang CH, Lin C, Ku CW. A high-efficiency solar array simulator implemented by an LLC resonant DC-DC converter. *IEEE Trans. on Power Electronics*. 2013;28(6):3039-3046.
6. Hayashi Y. Power density design of SiC and GaN DC-DC converters for 380 V DC distribution system based on series-parallel circuit topology. *28th Annual IEEE Applied Power Electronics Conference and Exposition*. 2013;1601-1606.
7. Wei C, Zhengyu L. Investigation on set of quasi-isomorphic topologies and structural variations of type-4 LLC resonant DC-DC converter based on modulefunction identification. *Proceedings of the CSEE*. 2009;29(9):35-42. (in Chinese).
8. Ma Hao, Qi Feng. An improved design method for resonant tank parameters of LLC resonant converter. *Proceedings of the CSEE* 2008,28(33): 6-11.(in Chinese).
9. Feng WY, Lee FC, Mattavelli P. Optimal trajectory control of burst mode for LLC resonant converter. *IEEE Trans. on Power Electronics*. 2013;28(1):457-466.
10. Hu Haibing, Wang Wanbao, Sun Wenjin, et al. Optimal efficiency design of LLC resonant converters. *Proceedings of the CSEE* 2013, 33 (18):48-56. (in Chinese).
11. Jin Ke, Ruan Xinbo. Hybrid full bridge three-level LLC resonant converter. *Proceedings of the CSEE* 2006, 26(3): 53-58. (in Chinese).
12. Noah M, Umetani K, Imaoka J, Yamamoto M. Lagrangian dynamics model and practical implementation of an integrated transformer in multi-phase LLC resonant converter. *IET Power Electron*. 2018;11(2):339-347.
13. Fu DB, Liu Y, Fred LC, et al. A novel driving scheme for synchronous rectifiers in LLC resonant converters. *IEEE Trans on Power Electronics*. 2009;24(5):1321-1329.
14. Lu B, Liu WD, Liang Y, et al. Optimum design methodology for LLC resonant converter. In *Proceeding of IEEE Applied Power Electronics Conference and Exposition*. 2006;533-538.
15. Yang B, Lee FC, Concannon M, et al. Over current protection methods for LLC resonant converter. In *Proceeding of IEEE Applied Power Electronics Conference and Exposition*. 2003;2:605-609.
16. Hua C-C, Fang Y-H, Lin C-W. LLC resonant converter for electric vehicle battery chargers. *IET Power Electron*. 2016;9(12):2369-2376.
17. Lin B-R, Chu C-W. Hybrid full-bridge and LLC converter with wide ZVS range and less output inductance. *IET Power Electron*. 2016;9 (2):377-384.
18. Severns R. Topologies for three element resonant converters. IEEE APEC 1990, Los Angeles, California, USA; 1990;7(1):89-98.
19. Malan WL, Vilathgamuwa DM, Walker GR. Modeling and control of a resonant dual active bridge with a tuned CLLC network. *IEEE Trans Power Electron*. 2016;31(10):7297-7310.
20. Zou SL, Lu JH, Mallik A, Khaligh A, Bidirectional CLLC. Converter with synchronous rectification for plug-in electric vehicles. *IEEE Transactions on Industry Applications*. 2018;54(2):998-1005.
21. Chaohui Liu, Jiabin Wang, K. Colombage et al. A CLLC resonant converter based bidirectional EV charger with maximum efficiency tracking. 8th IET International Conference on Power Electronics, Machines and Drives (PEMD 2016).2016;2016(cp684).
22. Sun L, Suo X, Hao J, Zhang J, Ma Y, Wang X. Modal computation and analysis based on phase sequence of LLC resonant DC-DC converter. *Mathematical Problems in Engineering*. 2019. <https://doi.org/10.1155/2019/1571609>
23. Lv Z, Yan X, Fang Y, Sun L. Mode analysis and optimum design of bidirectional CLLC resonant converter for high-frequency isolation of DC distribution systems. 2015 *IEEE Energy Conversion Congress and Exposition (ECCE)*. 2015;1513-1520.
24. Yu-bao X, Yu-cai X, Fang-hua Z, Chang-bao W. Bi-directional DC transformer based on full-bridge LLC resonant. *Power Electronics (in Chinese)*. 2013;47(4):3-5.
25. Qichao C, Yanchao J, Wang J. Analysis and design of two-way CLLC resonant DC transformer. *Proceedings of the CSEE*. 2014;34(18): 2898-2905. (in Chinese).

How to cite this article: Sun L, Ma Y, Wang J, Hao J, Suo X, Li X. Analysis and design of asymmetric CLLC resonant DC-DC converter. *Int Trans Electr Energy Syst*. 2020;30:e12338. <https://doi.org/10.1002/2050-7038.12338>